CHEMISTRY
A EUROPEAN JOURNAL

FULL PAPER

DOI: 10.1002/chem.201104023

1*H*-Azepine-4-amino-4-carboxylic Acid: A New α,α-Disubstituted Ornithine Analogue Capable of Inducing Helix Conformations in Short Ala-Aib Pentapeptides

Sara Pellegrino,* Alessandro Contini,* Francesca Clerici, Alessandro Gori, Donatella Nava, and Maria Luisa Gelmi[a]

Abstract: A very efficient synthesis of orthogonally protected 1*H*-azepine-4-amino-4-carboxylic acid, abbreviated as Azn, a conformationally restricted analogue of ornithine, was realized. It was obtained on a gram scale in good overall yield in five steps, three of which did not require isolation of the intermediates, starting from the readily available 1-amino-4-oxo-cyclohexane-4-carboxylic acid. Both enantiomers were used for the preparation of pentapeptide models containing Ala, Aib, and Azn. Conformational studies using both spectroscopic techniques (NMR, CD) and molecular dynamics on model 5-mer peptides showed that the (*R*)-Azn isomer possesses a marked helicogenic effect.

Keywords: conformation analysis · helical structures · molecular dynamics · peptidomimetics · protein folding

Introduction

The production of marketed synthetic peptide drugs is increasing yearly.[1] Indeed, their role as mediators of key biological functions and their unique intrinsic properties, such as high biological activity, low toxicity, and high specificity,[2] make them particularly attractive therapeutic agents. Nevertheless, the use of peptides containing natural amino acids is often associated with limitations related to their metabolic instability and low bioavailability. These drawbacks can be overcome by preparing peptidomimetics, molecules designed to mimic both the structural and biological features of peptides. As is widely known, many biological functions involve protein–protein interactions (PPIs), in which helical structured motifs often play a fundamental role as recognition elements. They are characterized by a central polypeptide backbone that serves to project, along individual faces, residues that mediate selective and specific recognition. The α-helix therefore offers potential as a template for the elaboration of "rule-based" small-molecule PPI inhibitors as artificial peptides and "foldamers", synthetic non-natural oligomers that adopt well-defined conformations reminiscent of protein secondary structure.[3]

Typically, preparations of backbone mimetics that reproduce the local topography of the helical pattern take advantage of α,α-disubstituted amino acids that dramatically reduce the available conformational space of the peptide backbone.[4] The main representative amino acid of this class is α-aminoisobutyric acid (Aib), which, like similar amino acids,[5] promotes the formation of α- or 3_{10}-helices,[6,7a] these being the two most prevalent helices found in proteins.

In the last decade, ever-increasing numbers of scientific contributions on the synthesis of α,α-disubstituted amino acids have appeared. In this context, numerous 1-amino-1-cycloalkanecarboxylic acids (Ac_nc, $n=3$–12) have been prepared, and have proved to be valuable in the preparation of conformationally constrained peptide backbones.[4,6,7a] On the contrary, few examples of α,α-disubstituted azacyclic amino acids, such as the achiral piperidine-4-amino-4-carboxylic acid (Api) and its derivatives, have been used in the preparation of peptides.[4b,e,7g,8,9]

Focusing on the azepino scaffold,[10] some 1*H*-azepine-3-amino-3-carboxylic acid derivatives have been prepared, most of them containing the lactam function. In three patent applications, 2-oxo derivatives and their benzo-condensates have been claimed for the preparation of oligopeptides useful as melanoma inhibitors,[11a] brain function improvers,[11b] or psycho analeptics.[12] Furthermore, the preparation of antimicrobial agents by using 1*H*-azepine-4-amino-4-carboxylic acid derivatives has been mentioned in another patent application,[13] while the synthesis of the corresponding 3-oxo derivatives has recently been reported.[14]

Our interest in the preparation of constrained amino acids is well documented,[15] especially carbocyclic α-amino

[a] Dr. S. Pellegrino, Dr. A. Contini, Prof. F. Clerici, Dr. A. Gori, D. Nava, Prof. M. L. Gelmi
DISMAB, Sezione di Chimica Organica "A. Marchesini"
Facoltà di Farmacia, Università degli Studi Milano
Via Venezian 21, 20133 Milano (Italy)
Fax: (+39) 02-50314476
E-mail: sara.pellegrino@unimi.it
alessandro.contini@unimi.it

Supporting information for this article is available on the WWW under http://dx.doi.org/10.1002/chem.201104023.

acids,[15b,c,e,f,i–o] and in this work we report the preparation of the conformationally constrained ornithine analogue 1*H*-azepine-4-amino-4-carboxylic acid **3**, abbreviated as Azn, and its use for the preparation of model peptidomimetics.

The key steps for obtaining **3** are shown in the retrosynthetic analysis (Scheme 1). Starting from the readily available amino acid **1**, containing a cyclohexanone scaffold, amino acid **3** was obtained via lactam intermediate **2**. Compound **3** was synthesized on a gram scale and orthogonally protected at its two nitrogen atoms, thus enabling its use for the preparation of model peptidomimetics. As azepino derivative **3** is chiral, its preparation represented an added value with respect to Api since different effects on the peptide conformation could be expected depending on the absolute configuration of the starting amino acid.[7d]

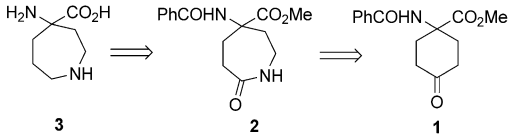

Scheme 1. Retrosynthetic scheme for 1*H*-azepine-4-amino-4-carboxylic acid.

Conformational studies using both spectroscopic techniques (NMR, CD) and molecular dynamics on model pentapeptides containing Ala, Aib, and Azn are also reported herein.

Results and Discussion

Synthesis of Azn: The starting material for the preparation of amino acid derivative **3** was the known keto compound **1**,[16] which was prepared according to the standard protocol on a multigram scale (40 g) and in good yield (80%). Starting from the keto derivative **1**, compound **2** was efficiently obtained by a modified Schmidt procedure that involved the addition of sodium azide (3 equiv) to a cooled solution (−10 °C) of **1** in $CHCl_3$ and in the presence of concentrated H_2SO_4 under stirring. Performing the reaction in a sealed round-bottomed flask was found to be crucial for achieving a good yield, as was stopping the stirring after 30 min and allowing the reaction mixture to warm to ambient temperature over 18 h. Pure lactam **2** could be obtained on a gram scale in 87% yield (Scheme 2).

Since compound **2** contains three carbonyl functions, selective reduction of the lactam function to the corresponding amino form was not trivial. Different procedures were investigated according to methods reported in the literature,[17–19] but a mixture of compounds or the starting material[20] was recovered. Positive results were achieved by selectively transforming the lactam **2** into thiolactam **4** using the Lawesson reagent (0.5 equiv) in CH_2Cl_2 at 60 °C.[21] Compound **4**, isolated in 81% yield, was then treated with Raney Ni in MeOH at reflux to afford the azepino compound **5** (83%). The reaction was found to be efficient when operating on a small scale (200 mg), but on a multigram scale (10 g) the yields were not reproducible. For this reason, we shifted toward the preparation of methyl isothiouronium salt **6**, obtained by reaction of **4** with MeI in THF,[22] which was not isolated but directly reduced with $NaBH_3CN$ in MeOH/AcOH (pH 5) to afford pure amine **5** (64%) (Scheme 3).

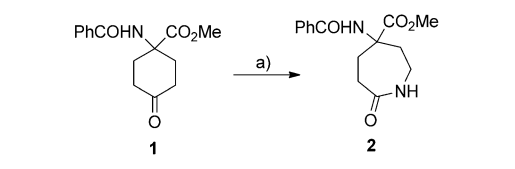

Scheme 2. a) H_2SO_4, NaN_3, $CHCl_3$, from −10 to 25 °C, 87%.

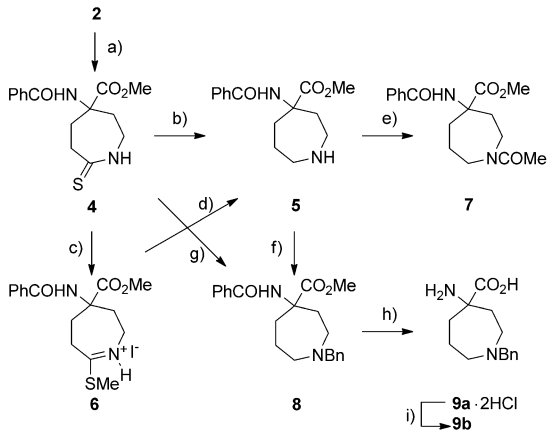

Scheme 3. a) The Lawesson reagent, CH_2Cl_2, Δ, 81%; b) on small scale: Raney Ni, MeOH, reflux, 83%; c) MeI, THF; d) $NaCNBH_3$, MeOH, AcOH, 64% over two steps; e) Ac_2O, TEA, THF, 90%; f) PhCHO, 1,2-dichloroethane, AcOH, $NaBH(OAc)_3$, 61%; g) c) then d) then f), 50%; h) 6 N HCl, reflux, quantitative yield; i) MeOH, propylene oxide, quantitative yield.

Analytical and spectroscopic data confirmed the selective reduction of the lactam function, although the ^1H NMR spectrum was complicated. With the aim of clarifying the possible presence of conformers, the *N*-acetyl derivative **7** was prepared (yield 90%) by reaction of **5** with acetic anhydride in the presence of triethylamine (TEA) in THF (Scheme 3).

The ^1H NMR spectrum of **7** in $CDCl_3$ at 25 °C revealed the presence of dual signals at $\delta = 6.53/6.39$ (NH), $\delta = 3.74/3.71$ (OMe), and $\delta = 2.05/1.99$ (Me), suggesting the presence of *E*/*Z* isomers about the tertiary amide bond. Dynamic NMR experiments (from 25 to 80 °C) in DMSO revealed coalescence of these pairs of signals at 80 °C, confirming the presence of *E*/*Z* isomers at room temperature.

As compound **5** was the key intermediate for the preparation of the target model peptide, orthogonal protection of its two nitrogen atoms was needed. By following a reductive amination approach, the *N*-benzylamine **8** was obtained in

61% yield by reacting compound **5** with benzaldehyde in 1,2-dichloroethane in the presence of acetic acid (pH 5, 30 min) and then adding $NaBH(OAc)_3$ and allowing the reaction to proceed for 12 h (Scheme 3). In order to improve the overall yield of **8** starting from **4**, we evaluated the possibility of directly obtaining the *N*-benzyl derivative **8** without the isolation of intermediates. The two reductive steps were then performed in a "one-pot" fashion, directly affording *N*-benzylamine **8** (50% instead of 38% yield).

Compound **8** was then transformed into amino acid **9a** by hydrolysis with 6N HCl (reflux, 8 h, quantitative yield). Free amine **9b** was isolated by treating **9a** with propylene oxide in MeOH (Scheme 3).

Synthesis of model pentapeptides: The use of the seven-membered-ring azepino amino acid **9** in peptide synthesis was explored. We planned the preparation of pentapeptide models containing Ala and Aib, in which the Azn residue was located at position i+1, that is, Fmoc-L-Ala-(*R*)-Azn-L-Ala-Aib-L-$AlaNH_2$ (**11a**) and Fmoc-L-Ala-(*S*)-Azn-L-Ala-Aib-L-$AlaNH_2$ (**11b**), differing only in the presence of the two Azn stereoisomers.

With the aim of separating the Azn enantiomers, we planned the synthesis of the dipeptide Ala-Azn by using L-alanine as both reagent and resolving agent following the methodology of Carpino et al.,[23] who exploited the high reactivity of acyl fluorides. First, the hydrochloride salt of racemic Azn **9a** was reacted with triethylsilyl chloride (2 equiv, CH_2Cl_2, reflux) allowing simultaneous protection of the carboxylic acid and activation of the nitrogen atom.[24] After 2 h, the reaction mixture was cooled and diisopropylethylamine (DIPEA) (5 equiv) and Fmoc-Ala-F (1.5 equiv) were added. A mixture of Fmoc-L-Ala-(*R*)-Azn (**10a**) and Fmoc-L-Ala-(*S*)-Azn (**10b**) was isolated in 45% yield. With the aim of avoiding the use of DIPEA, which hampers the purification of our basic dipeptides, we turned to the use of free amino acid **9b** in conjunction with bis-trimethylsilylacetamide (BSA, 4 equiv) as silylating agent.[25] The reaction was performed at 25°C (15 h) in CH_2Cl_2 in the presence of activated molecular sieves. The coupling reaction with Fmoc-L-Ala-F was immediate (10 min), affording Fmoc-L-Ala-(*R*)-Azn (**10a**) and Fmoc-L-Ala-(*S*)-Azn (**10b**) in an improved yield (70%). The two diastereoisomers were separable by flash column chromatography (Scheme 4).

The tripeptide Ala-Aib-$AlaNH_2$ was prepared on a solid phase using Rink amide resin (loading 0.8 mmol g^{-1}) as the solid support. The first Ala was loaded onto the resin under standard coupling conditions (5 equiv Ala, 5 equiv 1-hydroxybenzotriazole (HOBt), 5 equiv *O*-(benzotriazol-1-yl)-*N*,*N*,*N*′,*N*′-tetramethyluronium hexafluorophosphonate (HBTU), 10 equiv DIPEA). The Fmoc protecting group was removed by using 20% piperidine in DMF. Due to the steric hindrance of the methyl groups on C_α, the coupling efficiency of Aib and the residue at the Aib+1 position in the stepwise assembly of peptide chains is usually poor.[26] For this reason, we pre-activated both Aib and the adjacent Ala using *N*,*N*′-diisopropylcarbodiimide (DIC) and HOBt

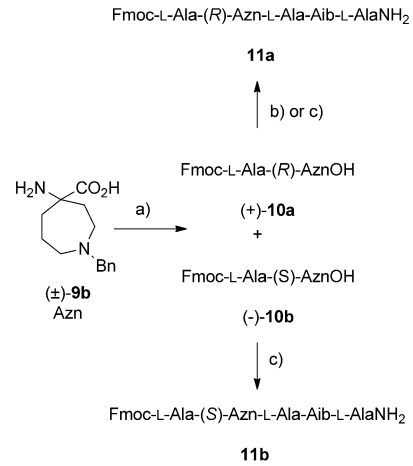

Scheme 4. a) BSA, molecular sieves in anhydrous CH_2Cl_2 for 15 h, then Fmoc-L-Ala-F for 10 min, 70%; b) HOAT, EDC in NMP for 1 h, then H_2N-L-Ala-Aib-L-Ala-$CONH_2$ for 15 h, 30%; c) H_2N-L-Ala-Aib-L-Ala-$CONH_2$, DCC in CH_2Cl_2, 48 h; **11a**: 50%, **11b**: 30%.

(20 min) before performing the coupling (Aib: 3 h; Ala: overnight). The tripeptide was then cleaved from the resin (TFA/H_2O/triisopropylsilane (TIS), 90:5:5) and purified by crystallization (Et_2O).

Finally, pentapeptide Fmoc-L-Ala-(*R*)-Azn-L-Ala-Aib-L-$AlaNH_2$ (**11a**) was prepared by solution-phase synthesis. Enantiopure Fmoc-L-Ala-(*R*)-AznOH (**10a**) was reacted with Ala-Aib-$AlaNH_2$ (3 equiv) according to a standard protocol (2 equiv 1-hydroxy-7-azabenzotriazole (HOAT), 1 equiv *N*-(3-dimethylaminopropyl)-*N*′-ethylcarbodiimide hydrochloride (EDC) in *N*-methylpyrrolidone (NMP), 25°C, 15 h). Pentapeptide **11a** was isolated in moderate yield (30%) together with recovered dipeptide **10a** (40%) after purification by RP-HPLC. Interestingly, the diastereoisomer Fmoc-L-Ala-(*S*)-AznOH (**10b**) was found to be dramatically less reactive in the coupling reaction. Indeed, by following the same protocol as described above, only the starting dipeptide was recovered and no product formation was detected. Various attempts were then made to obtain the desired pentapeptide **11b**. First, the coupling was attempted by using the already mentioned conditions with the aid of microwave irradiation (55°C, 400 W, 30 min), but no positive results were obtained. According to a known procedure,[7d] a mixture of activating reagents (HOAT, 2 equiv; HBTU, 1 equiv) in the presence of DIPEA (4 equiv) was used, but only after 5 days was a trace amount of **11b** obtained. A further attempt was made by converting the dipeptide **10b** into the corresponding more reactive acyl fluoride but, curiously, no reaction occurred. The conversion of **10b** into its acyl chloride equivalent with $SOCl_2$ also failed. Finally, better results were obtained when compound **10b** was reacted with the tripeptide Ala-Aib-$AlaNH_2$ using *N*,*N*′-dicyclohexylcarbodiimide (DCC) (1.5 equiv) as the coupling activator. The desired pentapeptide **11b** was thereby obtained in 30% yield. When the same procedure was applied to dipeptide **10a**, the product **11a** was obtained in 50% yield. From

these results, the difference in reactivity of the two diastereomeric dipeptides is clear, which can most probably be attributed to different degrees of exposure of the carboxylic group as a result of different hydrophobic interactions between the Fmoc and benzyl groups.

Unfortunately, all attempts to prepare crystals suitable for structure determination and an unequivocal assignment of the (*R*)/(*S*) configuration of Azn were unsuccessful. Although an NOE experiment on peptide **11a** provided a clear indication of (*R*)-Azn stereochemistry (see the section headed NMR spectroscopy studies), a proposed assignment should be considered in the following discussion.

Solution conformational analysis: To evaluate whether the Azn scaffold could stabilize a helical conformation, we performed conformational studies by CD and NMR.

CD measurements: The CD spectra of peptides **11a** and **11b** were recorded in MeOH (300 μM solutions) in the far-UV region (195–250 nm). As shown in Figure 1, in both cases, the presence of a positive band below 200 nm, a minimum in the region 205–210 nm (amide π→π* transition), and a shoulder at around 222 nm (amide n→π* transition) indicate the presence of right-handed helical structures. The *R* ratios ($\theta_{222}/\theta_{208}$) suggest that the dominant helical structure is the 3_{10}-helix (**11a**: $R=0.55$; **11b**: $R=0.5$), although for **11b** a blue shift of the π→π* band indicates the presence of different conformations as well as a disordered fraction. The lower intensity of the Cotton effect in peptide **11b** than in **11a** could be ascribed to the presence of a left-handed helix contribution, as suggested by the computational study described below. Furthermore, the Fmoc group can contribute in the far-UV region with a positive peak below 214 nm, suggesting that the helical contents of both peptides could be underestimated.[27] It should also be noted that previous studies on the conformational behavior of Ala-Aib-containing peptides have shown that a right-handed 3_{10}-helical structure usually first appears at the 7-mer level in MeOH.[5a] In the present case, we observed a helical conformation with a pentamer, suggesting that Azn has a strong helicogenic effect.

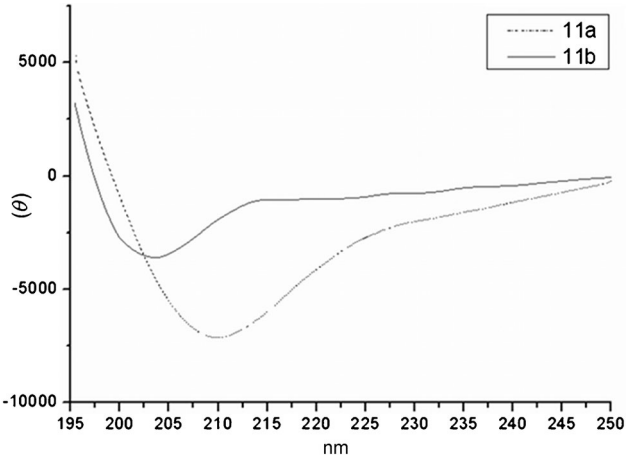

Figure 1. CD spectra in the 195–250 nm region of peptides **11a** and **11b**. The ellipticity is expressed as mean residue molar ellipticity, $[\theta]_R$/deg cm^2 dmol^{-1}.

NMR spectroscopy studies: Compared with CD, NMR spectroscopy techniques offer the advantage of monitoring peptide conformations at the level of the individual residues. In particular, dynamic NMR experiments can give information on H-bonded protons, while 2D experiments can reveal the spatial disposition of the peptide backbone.[28] As a further confirmation of the CD data, which indicated a prevalent right-handed 3_{10}-helix conformation for peptide **11a**, dynamic NMR experiments were also performed.

A full assignment of the protons of peptide **11a** (see Table S1 in the Supporting Information) was accomplished by 500 MHz NMR analysis (^{1}H, ^{13}C, COSY, HSQC, and HMBC NMR experiments). To obtain detailed information on the conformational preferences, 2D-NOESY at different mixing times, temperature-dependent chemical shift variations (from 0 to 60 °C), and deuterium exchange experiments were performed in CD_3CN solution.

As shown in Figure S3 (A and B) (in the Supporting Information), various NOEs are operative in pentapeptide **11a**. Medium to weak α,N(i,i+1) and α,N(i,i+3) NOEs (Figure 2(A)) as well as a complete set of N,N(i,i+1) NOE cross-peaks (except for Ala3, the NH signal of which falls in the aromatic region), which are characteristic of a helical conformation, were observed (Figure 2(B)). Medium β,N-(i,i+1) NOEs between residues 3/4 and 4/5 reinforce the hypothesis of a helical structure (Figure S3 (A), in the Supporting Information).[28]

Longer range α,N(i,i+2) and α,N(i,i+4) NOEs allow a distinction of the helix types: the former is typical of a 3_{10}-helix, while the latter is typical of an α-helix.[28] Our data support the prevalence of a 3_{10}-helix since the α,N(i,i+2) NOE is present in the structured helical fragment corresponding to Ala3/Ala5 (Figure 2A). Interestingly, a positive Overhauser effect was found between the methyl group of Ala5 and H2 of Azn (Figure S3 (B), in the Supporting Information), confirming not only the formation of a helical structure, but also that the absolute configuration of the amino acid Azn is (*R*). In fact, this NOE is forbidden in the case of the (*S*)-isomer (see Figure 5). Furthermore, the Fmoc moiety was seen to be in spatial proximity with the methyl group of Ala3 but not with the Azn moiety, thus confirming the formation of a hydrogen bond between NH-3 and the Fmoc carbonyl function that helps to orientate this group.

The temperature dependences of the NH proton chemical shifts, which provide information on inaccessible or intramolecular H-bonds,[29] were evaluated as -2 ppb K^{-1} for Ala3, -2.1 ppb K^{-1} for Aib, -1.7 ppb K^{-1} for Ala5, and -2.1 ppb K^{-1} for one of the lower-field protons of NH_2, which fall within the typical ranges for intramolecularly H-bonded protons (Figure 3). Conversely, an equilibrium be-

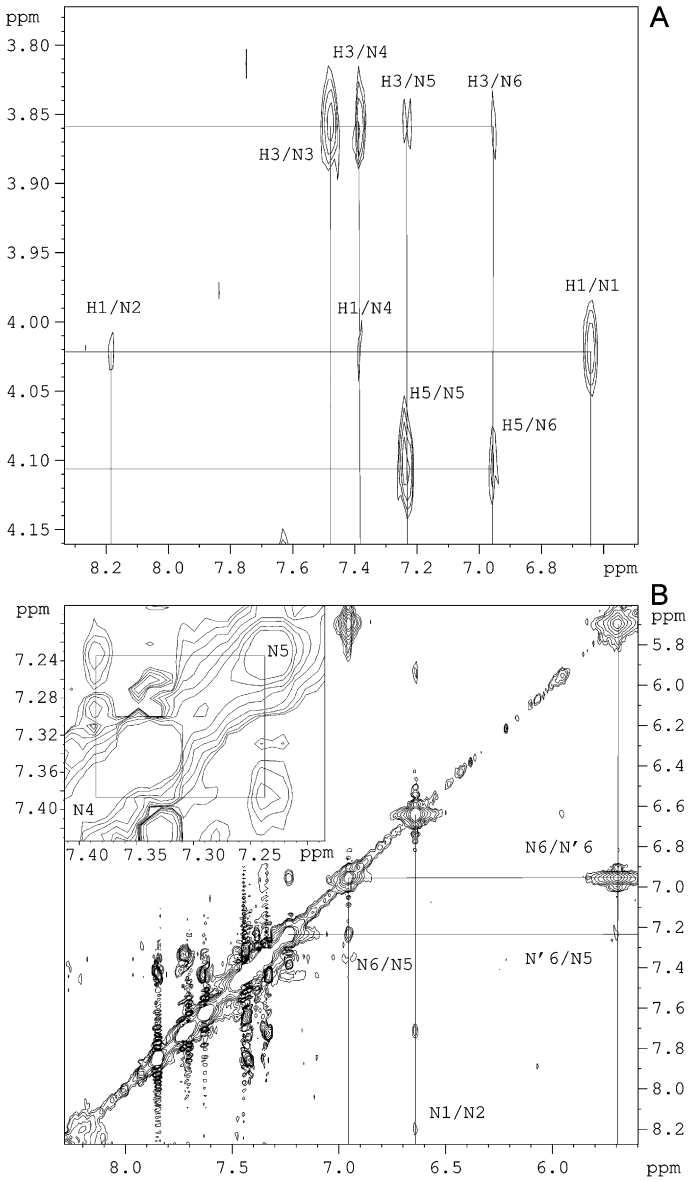

Figure 2. Sections of the NOESY spectrum of **11a** (10.41 mM solution in CD_3CN, 500 MHz, RT). A) CH/NH region and B) NH region.

tween an intramolecularly H-bonded and a non-H-bonded state is suggested for the NH moieties of Ala1 and Azn on the basis of temperature dependences of −5.6 and −6.8 ppb K^{-1}, respectively. These results were confirmed by NH/ND exchange experiments (0–70887 s; 10.4 mM). The exchange rate of H-5/D upon addition of D_2O proved to be very slow, with the signal of this proton still being present at the end of the experiment (about 40% deuterated). Due to partial overlap with the aromatic proton signals, the deuteration of NH-3 and NH-4 could not be quantitatively analyzed, although the relative integrals of the aromatic region at the beginning and end of the experiment did not show a significant decrease. In marked contrast, NH-1, NH-2, and both protons of NH_2 exchanged immediately.

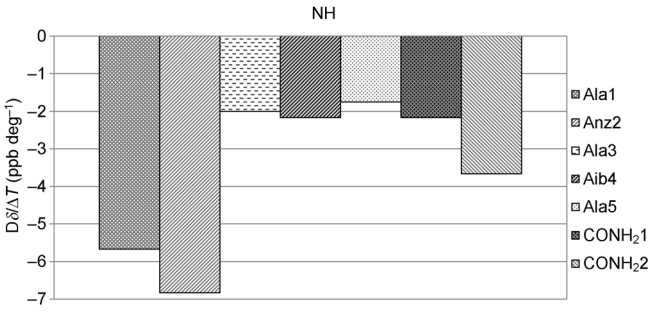

Figure 3. Plot of the variations of NH proton chemical shifts in the ^1H NMR spectra of **11a** as a function of increasing temperature (10.41 mM solution in CD_3CN, 300 MHz, 273–333 K).

From the above experiments, it is evident that the chemical shifts of two protons, NH-1 and NH-2, are remarkably sensitive to heating, and that these protons readily undergo exchange with deuterium. On the contrary, the observations for NH-3, NH-4, and NH-5 are consistent with overwhelmingly intramolecularly H-bonded protons. As regards the NH_2 group, the variable-temperature experiment revealed the involvement of the proton resonating at lower field in a hydrogen-bond, even though the same proton was exchanged very quickly.

All of the above data suggest that a 3_{10}-helix construct is present at the C-termini and that the hydrogen bonds involving NH-3, NH-4, NH-5, and NH-6 are preserved up to 60 °C.[7d,29]

Computational analysis: To gain a deeper knowledge about the folding preferences of the (*R*)- and (*S*)-Azn-based peptides **11a**,**b**, we planned a molecular dynamics (MD) study of pentapeptides containing L-Ala at positions 1, 3, and 5, (*R*)-Azn or (*S*)-Azn at position 2, and Aib at position 4, using the Amber11 package.[30]

The replica exchange molecular dynamics (REMD) method,[31] a generalized-ensemble algorithm performing random walks in energy space, thus helping a system to escape from local energy traps, has been successfully adopted in secondary structure predictions due to its improved sampling capabilities over standard MD runs. Recent literature evidences several successful applications of REMD for the prediction of the native structures of small proteins such the Villin headpiece domain HP35,[32] the pin WW domain,[33] Trp-cage,[34] and GB1 peptide.[35] There have been fewer instances of the use of MD to study the folding of peptides containing non-natural amino acids.[36] Among non-natural amino acids, the best studied is Aib, the tendency of which to induce 3_{10}-helix formation has been correctly evidenced by MD simulations.[36b,c] When dealing with peptide folding, the choice of an appropriate combination of force-field type and solvent model appears to be critical.[37] For instance, the popular Amber force fields ff03 and f99 have shown a strong bias toward helical structures,[38a,b] while ff99SB has proved to be promising in ab initio folding experiments,[38c,d] due to its lower α-helical propensity.[38a]

The force-field behavior can be strongly influenced by the adopted solvent model. In this framework, Shell and coworkers[37] recently reported a study aiming to identify the force field/solvation model combination best able to reproduce the α-helix or β-hairpin native structure of four 12- to 16-mer proteins, and concluded that the ff96 force field and the Generalized Born (GB) solvation model with the atomic radii of Onufriev, Bashford, and Case (igb = 5)[39,40] provided a correct balance of α-helical and β-hairpin tendencies of the tested peptides. The ff99SB/igb = 5 combination also performed well in predicting helical conformations, but was less accurate for β-hairpins. However, in the aforementioned studies, no peptides adopting different helical structures, such as the 3_{10}- and polyproline (PPII) helices, were investigated. Moreover, the relative performances of force-field-based methods might be affected by the presence of non-natural amino acids. For these reasons, and considering that due to computational limitations we preferred implicit as opposed to explicit solvation, we decided to evaluate both the ff96 and the ff99SB force fields coupled with the igb = 5 solvent model. Several sets of experimental data were available for Aib- and Ala-containing peptides,[5a,6c,d] but the 5-mer Ala-Aib-Ala-Aib-Aib was particularly well suited for our testing because its crystal structure, evidencing a 3_{10}-helical conformation, has been solved.[6c] The N- and C-termini were capped with acetyl (Ac) and NHMe groups instead of *t*Boc and OMe, respectively, as parameters for these residues are not present in the adopted force fields; the resulting model peptide is hereinafter referred to as P1. REMD simulations, consisting of 12 replicas with temperatures exponentially spaced between 260 and 660 K, were performed starting from unfolded conformations (see the Supporting Information for details). The peptide was simulated for 50 ns, and H-bond, geometrical, and clustering analyses were performed on the final 25 ns of the 308.5 K trajectory, this temperature most closely resembling the experimental conditions. Representative structures resulting from clustering analyses of the ff96 and ff99SB trajectories are compared in Figure S5 in the Supporting Information.

By analyzing the occupancies of selected H-bonds (Table 1), it can be observed that H-bonds characteristic of the expected 3_{10}-helix (i+3→i) are only observed with the ff99SB force field, together with a modestly persistent H-bond typical of α-helices (1+4→i). On the other hand, with the ff96 force field, an H-bond pattern compatible with the reported crystal structure cannot be observed. Moreover, a cluster analysis, performed by grouping coordinate frames by mass-weighted root-mean-square-deviation (rmsd) (Table 2, Table S2, and Figure S5 in the Supporting Information), showed that with the ff99SB force field the most populated cluster (pop. = 44.0 %) corresponded to the expected 3_{10}-helix. Two partially folded conformations (clusters #2 and #3, pop. = 31.0 and 13.2 %, respectively) and a small amount of left-handed helix (cluster #4, pop. = 6.9 %) were also identified. On the contrary, predominantly unfolded conformations were obtained with ff96, with the most populated cluster (pop. = 35.7 %) corresponding to an almost completely extended conformation. These calculations showed that, at least for the case reported herein, only the ff99SB force field coupled with the igb = 5 solvation model provided results consistent with the reported crystal structure, and hence this combination was adopted for the following calculations.

Table 1. H-bond[a] analysis of the final 25 ns of the 308.5 K REMD trajectory for P1 with ff96/igb = 5 and ff99SB/igb = 5 combinations.

H-bonds	ff96 Occupancy [%]	ff99SB Occupancy [%]
Ala1 C=O···HN Aib4	3.1	41.4
Ala1 C=O···HN Aib5	10.6	7.5
Aib2 C=O···HN Aib5	2.6	21.7

[a] Only H-bonds with an occupancy > 1 % are reported. H-bonds involving the capping Ac and NHMe groups are not reported.

Table 2. Cluster analysis[a] of the final 25 ns of the 308.5 K REMD trajectory for P1 with ff96/igb = 5 and ff99SB/igb = 5 combinations.

#	ff96 pop [%]	ff96 φ, ψ_{avg}[b]	ff99SB pop [%]	ff99SB φ, ψ_{avg}[b]
1	35.7	−45.7 ± 74.1, 54.7 ± 155.1	44.0	−50.6 ± 9.6, −33.7 ± 11.7
2	22.7	13.9 ± 77.7, 1.8 ± 157.1	31.0	−22.4 ± 87.2, −20.9 ± 45.9
3	20.7	−53.8 ± 19.1, 7.1 ± 114.0	13.2	18.5 ± 65.7, 85.6 ± 77.0
4	17.8	−13.0 ± 80.4, 66.2 ± 110.3	6.9	46.0 ± 8.1, 56.8 ± 49.9

[a] Results for the most populated clusters, covering above 95 % of the total population, are reported. [b] Average φ and ψ dihedrals (°) are obtained for each cluster representative structure by averaging the corresponding values for all residues, without the capping Ac and NHMe groups.

Analogous REMD simulations were then run for Ac-Ala-(*R*/*S*)-Azn-Ala-Aib-Ala-NMe peptides (hereafter referred to as P2 and P3, respectively). Trajectories were analyzed in terms of H-bonds (Table 3), 3D-Ramachandran plots, in which the Cartesian *z*-coordinate represents the frequency of occurrence of a particular combination of φ and ψ dihedrals (Figure 4 and Figure S7 in the Supporting Information), and cluster analyses (Table 4 and Figure 5 and Table S2 and Figure S8 in the Supporting Information).

Table 3. H-bond[a] analysis of the final 25 ns of the 308.5 K ff99SB REMD trajectory for P2 and P3 pentapeptides.

H-bonds	P2 (*R*)-Azn2 Occupancy [%]	P3 (*S*)-Azn2 Occupancy [%]
Ala1 C=O···HN Aib4	39.4	26.5
Ala1 C=O···HN Ala5	7.2	3.5
Azn2 C=O···HN Ala5	13.6	12.5

[a] Only H-bonds with an occupancy > 1 % are reported. H-bonds involving the capping Ac and NHMe groups are not reported.

As is evident from the H-bond analysis (Table 3), the (*R*)-Azn-containing peptide is characterized by two i+3→i H-bonds, which are typical of 3_{10}-helices, between residues 1–4 (Ala and Aib, respectively) and 2–5 (Azn and Ala, respectively). The third observed H-bond is of the i+4→i type, in-

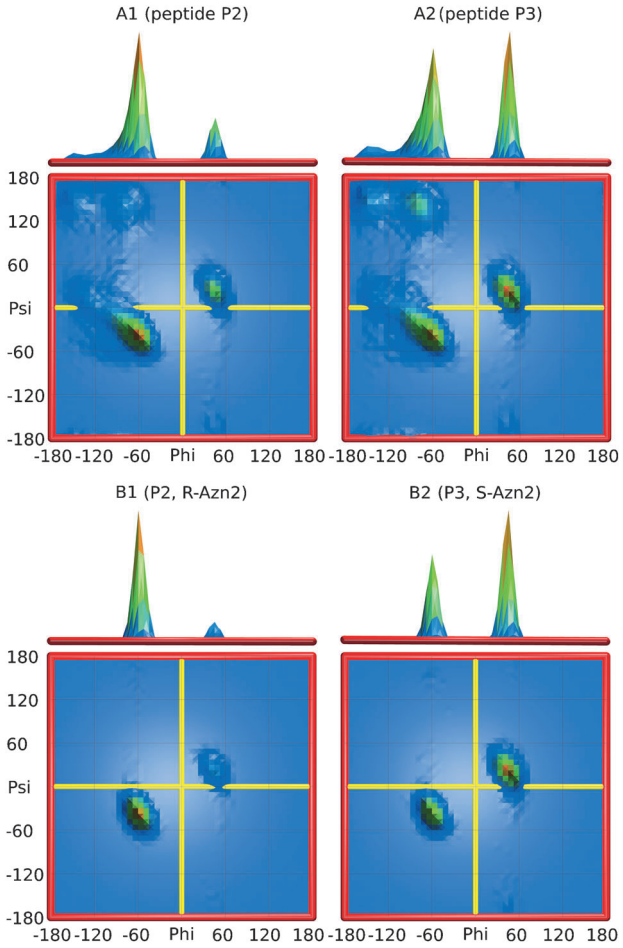

Figure 4. 3D Ramachandran plots for Ac-Ala-(*R*)-Azn-Ala-Aib-Ala-NMe (P2) and Ac-Ala-(*S*)-Azn-Ala-Aib-Ala-NMe (P3). The *z*-axis represents the frequency of occurrence. A: 3D plots for average φ and ψ dihedrals for the whole peptide. B: 3D plots for φ and ψ dihedrals for the sole residue 2 ((*R*)-Azn or (*S*)-Azn).

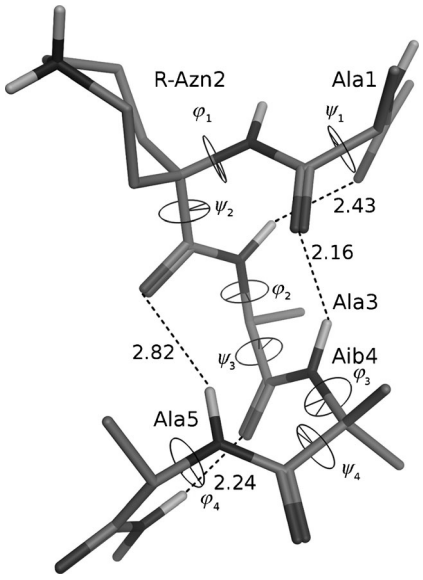

Figure 5. Cluster #1 representative structure as obtained from cluster analysis of the 308.5 K REMD trajectory of Ac-Ala-(*R*)-Azn-Ala-Aib-Ala-NMe peptide. C=O···HN distances are shown in angstroms. Selected geometrical parameters (°): $\psi_1 = -22.1$, $\varphi_1 = -30.7$, $\psi_2 = -52.7$, $\varphi_2 = -73.3$, $\psi_3 = -24.5$, $\varphi_3 = -57.7$, $\psi_4 = -32.2$, $\varphi_4 = -104.1$.

Table 4. Cluster analysis[a] of the final 25 ns of the 308.5 K ff99SB REMD trajectory for P2 and P3 pentapeptides.

	P2 (*R*)-Azn2		P3 (*S*)-Azn2	
#	pop [%]	φ, ψ_{avg}[b]	pop [%]	φ, ψ_{avg}[b]
1	44.7	-66.5 ± 30.7, -32.9 ± 13.9	54.2	-58.6 ± 72.0, 75.8 ± 90.9
2	42.9	-42.8 ± 64.2, -8.0 ± 25.5	35.6	-41.5 ± 58.7, -0.5 ± 57.4
3	7.4	-53.2 ± 67.9, 42.7 ± 78.0	7.6	18.0 ± 60.6, 51.3 ± 46.4

[a] Results for the most populated clusters, covering above 95% of the total population, are reported. [b] Average φ and ψ dihedrals (°) are obtained for each cluster representative structure by averaging the corresponding values for all residues, without the capping Ac and NHMe groups.

dicating an α-helix, and has an occupancy of 7.2%, suggesting that this secondary structure is also occasionally sampled. For the peptide P3, having (*S*)-Azn at the 2-position, a lower occupancy was observed for both the 1–4 and 1–5 H-bonds, while a comparable occupancy was observed for the 2–5 H-bond. In conclusion, H-bond analysis revealed a similar behavior for peptides P1 and P2, both of which show a preference for 3_{10}-helices, while for the (*S*)-Azn-containing peptide P3 a minor tendency for adopting helical configurations was observed, although definitive conclusions could not be drawn from this analysis.

More details were provided by an analysis of the 3D Ramachandran plots. Concerning the peptide P1 used as the reference (see Figure S6 in the Supporting Information), it is important to note that the Ramachandran plots obtained here for the Aib residues are consistent with those reported by Schweitzer-Stenner and co-workers for the tripeptide Ac-Ala-Aib-Ala-OMe.[36c]

Analysis of 3D Ramachandran plots for pentapeptide P2 (Figure 4 and Figure S7 in the Supporting Information) showed that, for the chiral (*R*)-Azn residue, the angles φ and ψ were mostly confined to the right-handed helix region ($-80° \le \varphi \le -30°$, $-60° \le \psi \le 0°$, with sharp peaks at $-55° \le \varphi \le -65°$ and $-30° \le \psi \le -40°$, Figure 4B1). This is in contrast to what was observed for P1-Aib2, which sampled both the right- and left-handed helices to similar extents. The 3D Ramachandran plot obtained for the whole peptide (Figure 4A1) also supported this observation, showing a clear preference for the right-handed over the left-handed helix; the latter is also present, but in a much lower amount than in the case of the peptide P1 (Figure S6 in the Supporting Information).

The behavior of P3 is substantially different. The conformational space explored by (*S*)-Azn (Figure 4B2) is indeed predominately in the left-handed helix region, with sharp peaks at $35° \le \varphi \le 45°$ and $20° \le \psi \le 30°$, and only a minor contribution from the right-handed helix region. These findings further confirm that the behavior of Azn, and hence its

ability to induce a certain secondary structure, is strongly dependent on its stereochemical configuration.

The findings are in excellent accordance with the experimental CD results, which indicated a prevalent helical secondary structure for the (*R*)-Azn2-containing peptide **11a**, but mixed or unordered conformations for the (*S*)-Azn2-containing peptide **11b**. Following on from the above discussion, we can conclude that (*R*)-Azn behaves as an L-amino acid and best exerts its helix-inducing capability when inserted into a sequence containing predominantly L-amino acids, such as that of **11a**. On the other hand, (*S*)-Azn behaves as a D-amino acid and its capability of inducing left-handed helices can only be properly exerted in a peptide containing D-amino acids, otherwise a prevalence of unordered structures or mixtures of right- and left-handed helices will be produced, as observed experimentally for **11b**.

A final confirmation was obtained by a cluster analysis of the REMD trajectories. As indicated in Table 4 and Table S2 in the Supporting Information, the first three most populated clusters represented over 95% of the total population for both peptides P2 and P3.

Concerning P2, the angles φ and ψ for the representative structure of cluster #1 (pop. = 44.7%) fall within the 3_{10}-helix region, with a significant deviation only for the φ_4 dihedral angle of the *C*-terminal Ala5 (Figure 5). Interestingly, cluster #2 (Table S2 and Figure S8 in the Supporting Information), which is also well populated (pop. = 42.9%), corresponds to a partially folded structure in which the φ and ψ values for residues 1–3 are appropriate for a right-handed helix, while the φ and ψ dihedrals for Aib4 fall in the left-handed helix region, analogously to what was observed for the reference peptide P1 (Table S2 and Figure S5 in the Supporting Information). Cluster #3 is only populated to a minor extent (pop. = 7.4%) and corresponds to an unfolded conformation.

For the (*S*)-Azn2-containing peptide P3, cluster #1 (pop. = 54.2%) corresponds to an unfolded conformation, while a structuring into a poorly defined helical conformation can be observed for cluster #2 (pop. = 35.6%). As also observed for P1, a minor contribution from the left-handed helix conformation is observed for the least populated cluster #3 (pop. = 7.6%).

Taken together, in accordance with the reported CD experimental results, the above data confirm that only (*R*)-Azn has a strong helicogenic effect when inserted in a short Ala- and Aib-containing sequence, while its enantiomer (*S*)-Azn, under the same conditions, is unable to induce a well-defined secondary structure.

Conclusion

Starting from the known keto amino acid **1**, a very efficient synthesis of orthogonally protected racemic amino acid **9**, a constrained analogue of ornithine, has been accomplished. The use of L-alanine as reagent and resolving agent allowed the preparation and isolation of pure diastereoisomeric dipeptides Fmoc-L-Ala-(*R*)-Azn and Fmoc-L-Ala-(*S*)-Azn, which were transformed into the pentapeptides Fmoc-L-Ala-(*R*)-Azn-L-Ala-Aib-L-AlaNH$_2$ (**11a**) and Fmoc-L-Ala-(*S*)-Azn-L-Ala-Aib-L-AlaNH$_2$ (**11b**).

It has been shown that the stereochemistry at C_α plays an important role in determining the folding preferences of Azn-containing peptides. Both computational and spectroscopic data revealed the capability of (*R*)-Azn to direct the folding of short peptide **11a** toward a well-defined 3_{10}-helix secondary structure. For this reason, we believe that Azn might be used for the rational design of non-natural peptides or peptidomimetic tools, leading to a finer and highly specific modulation of biochemical pathways. Further studies will be oriented towards evaluating the behavior of (*S*)-Azn in D-amino acid peptides, as it might prove to be a potent tool for the design of left-handed-helix peptides or peptidomimetics.

Experimental Section

General: Chemicals were obtained from Sigma-Aldrich and used without further purification. Fmoc-protected amino acids and Fmoc-Rink amide resin were purchased from Iris Biotech. RP-HPLC analyses were carried out on JASCO BS-997–01 equipment. Preparative RP-HPLC analyses were performed using a DENALI C-18 column from GRACE VYDAC (10 μm, 250×22 mm). Two mobile phases were used: A = 94.9% water, 5% MeCN, 0.1% TFA; B = 95% MeCN, 4.9% water, 0.1% TFA. ESI mass spectra were recorded on an LCQ Advantage spectrometer from Thermo Finnigan. CD spectra were recorded using a JASCO J-810 spectropolarimeter.

NMR spectroscopic analysis: NMR spectroscopic experiments were carried out on either a Varian MERCURY 200 MHz (200 and 50 MHz for ^{1}H and ^{13}C, respectively) or a Bruker Avance 500 MHz spectrometer (500 and 125 MHz for ^{1}H and ^{13}C, respectively). To take advantage of the magnetic field value, measurements that required temperatures higher than room temperature for observing coalescence were performed in an apparatus with a ^{1}H resonance frequency of 300 MHz (Bruker Avance 300 MHz spectrometer). 2D-NOESY experiments on peptide **11a** were performed at different mixing times (300, 600, 900 ms). Chemical shifts δ are given in ppm relative to $CHCl_3$ or CD_3CN as internal standards, and coupling constants *J* are reported in hertz (Hz).

Methyl 5-benzoylamino-2-oxa-azepan-5-carboxylate (2): Keto compound **1** (3 g, 10.9 mmol) was dissolved in $CHCl_3$ (45 mL) and the solution was cooled to −10 °C under vigorous stirring. 98% H_2SO_4 (1.75 mL) was added dropwise and then NaN_3 (2.2 g, 32.7 mmol) was added in small portions over a period of 20 min. The reaction mixture was allowed to warm to 25 °C over 30 min, then the stirring was stopped and the mixture was left for 18 h (TLC: CH_2Cl_2/MeOH, 10:1). The reaction was then quenched with ice (5 g) and the mixture was neutralized to pH 7 with 2 N NaOH. The layers were separated and the aqueous phase was extracted with CH_2Cl_2 (3×30 mL). The combined organic layers were dried over Na_2SO_4. After evaporation of the solvent, the crude product crystallized to afford pure compound **2** (2.8 g, 87%) as a white solid. M.p. 90–92 °C (Et_2O); ^{1}H NMR (200 MHz, $CDCl_3$, 25 °C): δ = 7.78–7.75 (m, 2H), 7.59–7.41 (m, 3H), 6.28 (s, 1H, exch.), 5.30 (t, *J* = 7.2 Hz, 1H, exch.), 3.77 (s, 3H), 3.46–3.36 (m, 2H; H-7), 2.75–2.40 (m, 2H; H-3), 2.75–2.35 (m, 2H; H-6), 2.35–2.25 ppm (m, 2H; H-4); ^{13}C NMR (50 MHz, $CDCl_3$, 25 °C): δ = 178.0, 174.3, 168.3, 134.4, 132.6, 129.2, 127.8, 61.9 (C-5), 53.4 (OMe), 37.8 (C-7), 36.4 (C-3), 31.0 (C-6), 30.4 ppm (C-4); IR (CH_2Cl_2): $\tilde{\nu}$ = 3291, 1737, 1650 cm^{-1}; MS (APCI): *m/z*: 291.1 $(M+1)^+$; elemental analysis calcd (%) for $C_{15}H_{18}N_2O_4$: C 62.06, H 6.25, N 9.65; found: C 61.80, H 6.51, N 9.37.

Methyl 5-benzoylamino-2-thioxa-azepan-5-carboxylate (4): Compound **2** (10 g, 35 mmol) was dissolved in CH_2Cl_2 (100 mL) and the Lawesson reagent (7 g, 17.4 mmol) was added. After sealing in a tube, the mixture was kept at 60 °C under stirring for 12 h (TLC: CH_2Cl_2/MeOH, 10:1). After evaporation of the solvent, the crude mixture was purified by chromatography on silica gel (cyclohexane/AcOEt, 100:1 to 2:1). Pure compound **4** (8.8 g, 81 %) was isolated as a pale-yellow solid. M.p. 226 °C (dec.; Et_2O); ^{1}H NMR (200 MHz, $CDCl_3$, 25 °C): $\delta = 8.60$ (s, 1H, exch.), 7.81–7.77 (m, 2H), 7.55–7.44 (m, 3H), 6.45 (s, 1H, exch.), 3.77 (s, 3H), 3.57–3.53 (m, 2H; H-7), 3.14–3.08 (m, 2H; H-3), 2.47–2.35 (m, 2H; H-6), 2.35–2.20 ppm (m, 2H; H-4); ^{13}C NMR (50 MHz, $CDCl_3$, 25 °C): $\delta =$ 208.5, 173.6, 167.9, 133.9, 132.6, 129.1, 127.5, 61.5 (C-5), 53.3 (OMe), 42.0 (C-7), 38.7 (C-3), 34.4 (C-6), 32.4 ppm (C-4); IR (KBr): $\tilde{\nu} = 3436$, 1735, 1645 cm^{-1}; MS (APCI): m/z: 307.1 $(M+1)^+$; elemental analysis calcd (%) for $C_{15}H_{18}N_2O_3S$: C 58.80, H 5.92, N 9.14; found: C 58.53, H 6.12, N 8.87.

Methyl 4-benzoylamino-azepan-4-carboxylate (5): *Method A*: Compound **4** (200 mg, 0.693 mmol) was dissolved in MeOH (4 mL) and Raney Ni (7.7 g of a methanolic slurry) was added. The mixture was heated at reflux for 2 h (TLC: CH_2Cl_2/MeOH, 10:1). After filtration through a bed of Celite, the solvent was removed and the crude mixture was purified by chromatography on silica gel (CH_2Cl_2/MeOH, 50:1 to 5:1 + 0.1 % NH_4OH) to afford pure **5** (150 mg, 83 %). *Method B*: MeI (2.1 mL, 30.8 mmol) was added to a solution of compound **4** (4.8 g, 15.4 mmol) in anhydrous THF (70 mL). The mixture was stirred at 25 °C for 8 h to form the solid isothiouronium salt **6**. After evaporation of the solvent, the crude mixture was used directly in the reductive step without further purification. MeOH (50 mL), AcOH (0.9 mL, to attain pH 5), and $NaBH_3CN$ (650 mg, 10.2 mmol) were added sequentially, and stirring was continued at 25 °C for 10 h, after which **6** had dissolved (TLC: CH_2Cl_2/MeOH, 10:1). 2 N HCl was added dropwise until pH 1 was attained, and the aqueous layer was washed with CH_2Cl_2 (20 mL). 2 N NaOH was added to the aqueous layer until pH 8 was attained. After evaporation of the solvent, the crude mixture was purified by chromatography on silica gel (CH_2Cl_2/MeOH, 50:1 to 5:1 + 0.1 % NH_4OH). Pure amine **5** (2.8 g, 64 %) was obtained as a colorless solid after crystallization. M.p. 190 °C (dec.; MeOH/Et_2O); ^{1}H NMR (200 MHz, CD_3OD, 25 °C): $\delta = 7.87$–7.81 (m, 2H), 7.60–7.40 (m, 3H), 3.72 (s, 3H), 3.42–3.29 (m, 4H; H-2, H-7), 2.90–2.70 (m, 1H), 2.65–2.44 (m, 1H), 2.44–2.22 (m, 2H), 2.18–1.80 ppm (m, 2H; H-6); ^{13}C NMR (500 MHz, [D$_6$]DMSO, 25 °C): $\delta = 174.2$, 169.6, 133.8, 131.9, 128.4, 127.5, 61.5 (C-4), 52.1 (OMe), 47.0 (C-7), 41.5 (C-2), 34.9 (C-5), 31.8 (C-3), 20.5 ppm (C-6); IR (KBr): $\tilde{\nu} = 3435$, 1733, 1635 cm^{-1}; MS (APCI): m/z: 277.3 $(M+1)$; elemental analysis calcd (%) for $C_{15}H_{20}N_2O_3$: C 65.20, H 7.30, 10.14; found: C 65.00, H 7.48, N 9.95.

Methyl 1-benzyl-4-benzoylamino-azepan-4-carboxylate (8): *Method C*: Amine **5** (1.4 g, 4.9 mmol) was added to 1,2-dichloroethane (25 mL) and a few drops of MeOH were added until complete dissolution of the reagent. AcOH (0.44 mL, 4.9 mmol) and benzaldehyde (578 mg, 6.4 mmol) were added and the mixture was stirred for 30 min, after which $NaBH(OAc)_3$ (1.9 g, 8.9 mmol) was gradually added over a period of 20 min. The reaction mixture was stirred overnight (TLC: CH_2Cl_2/MeOH, 10:1). 2 N HCl was added dropwise until pH 1 was attained and then 2 N NaOH was added until pH 8 was attained. The phases were separated and the aqueous layer was extracted with AcOEt (3×25 mL). The combined organic extracts were dried over Na_2SO_4. After evaporation of the solvent, the crude mixture was purified by chromatography on silica gel (cyclohexane/AcOEt, 10:1 to 1:2). *N*-Benzylamine **8** was obtained as a colorless oil (1.1 g, 61 %). *Method D*: Compound **8** (1.21 g, 50 % overall yield) was directly obtained from amine **5**, which was obtained from **4** (2.4 g, 7.7 mmol) according to *Method B*. After evaporation of the solvent, the crude mixture was subjected to *Method C* to afford *N*-benzylamine **8**, which was isolated as a colorless oil after purification on silica gel. Mixture of conformers: ^{1}H NMR (200 MHz, $CDCl_3$, 25 °C): $\delta = 7.82$–7.78 (m, 2H), 7.57–7.40 (m, 3H), 7.25 (s, 5H), 7.15 (s, 1H, exch.), 3.72 (s, 3H), 3.60 (s, 2H), 2.92–2.70 (m, 2H; H-7, H-2), 2.70–2.00 (m, 6H; H-7, H-2, H-5, H-3), 1.80–1.60 ppm (m, 2H; H-6); ^{13}C NMR (50 MHz, $CDCl_3$, 25 °C): $\delta = 174.6$, 167.1, 134.3, 131.9, 129.4, 129.2, 128.7, 128.6, 127.5, 127.4, 63.8 (CH_2Ph), 61.7 (C-4), 56.4 (C-7), 52.7 (OMe), 51.4 (C-2), 34.1 (C-5), 32.1 (C-3), 24.7 ppm (C-6); IR (KBr): $\tilde{\nu} = 3435$, 1738, 1639 cm^{-1}; MS (APCI): m/z: 367.2 $(M+1)^+$; elemental analysis calcd (%) for $C_{22}H_{26}N_2O_3$: C 72.11, H 7.15, N 7.64; found: C 71.73, H 7.40, N 7.31.

4-Amino-1-benzyl-azepan-4-carboxylic acid (9): Compound **8** (2.2 g, 6.0 mmol) was suspended in HCl (6 N, 25 mL). After sealing in a tube, the mixture was stirred at 120 °C for 8 h. After cooling, the precipitated solid was filtered off. The aqueous phase was washed with Et_2O (2× 20 mL) and then concentrated to dryness to afford **9a** (2 g) in quantitative yield. Salt **9a** was then suspended in MeOH (50 mL), and propylene oxide (500 μL, 7.2 mmol) was added. The mixture was stirred and heated under reflux for 1 h. The solvent was then evaporated and the crude residue was crystallized from Et_2O to afford free amino acid **9b** (1.5 g) in quantitative yield. **9a**: Mixture of conformers: M.p. 195 °C (MeOH/Et_2O); ^{1}H NMR (200 MHz, D_2O, 25 °C): $\delta = 7.47$ (br s, 5H), 4.34 (s, 2H; PhCH_2), 3.60–3.35 (m, 3H; H-2, H-7), 3.17–3.10 (m, 1H; H-7), 2.69–1.97 ppm (m, 6H; H-3, H-5, H-6); ^{1}H NMR (D_2O, 90 °C): $\delta = 8.20$ (s, 5H), 5.06 (s, 2H; PhCH_2), 4.30–4.14 (m, 2H; H-2), 4.14–4.00 (m, 2H; H-7), 3.35–3.26 (m, 1H; H-3), 3.15–2.96 (m, 2H; H-3, H-5), 2.84–2.72 ppm (m, 3H; H-6, H-5); ^{13}C NMR (50 MHz, D_2O, 25 °C): $\delta = 173.6$, 131.4 (131.2), 130.5, 129.5, 129.0 (128.9), 61.4 (61.3, *C*Ph), 61.2 (60.8, C-4), 56.3 (C-7), 49.4 (49.3, C-2), 33.3 (33.8, C-5), 30.1 (30.6, C-3), 19.6 ppm (20.6, C-6). Detected signals for the second conformer: ^{1}H/^{13}C NMR (D_2O, 27 °C): $\delta = 3.53$, 3.13 ($\delta = 56.3$, CH_2-7), 3.60, 3.39 ($\delta = 49.3$, CH_2-2), 2.64, 2.30 ($\delta = 30.6$, CH_2-3), 2.40, 1.98 ($\delta = 33.8$, CH_2-5), 2.02 ppm ($\delta = 20.6$, C-6); IR (KBr): $\tilde{\nu} = 3435$, 1726, 1631 cm^{-1}; ESI: m/z: 249.5 $(M+1)^+$; elemental analysis calcd (%) for $C_{14}H_{22}Cl_2N_2O_2$: C 52.34, H 6.90, N 8.72; found: C 51.95, H 7.30, N 8.41. **9b**: M.p. 188 °C (MeOH/*i*Pr_2O); ^{1}H NMR (200 MHz, CD_3OD, 25 °C): $\delta = 7.55$–7.47 (m, 5H), 4.36 (s, 2H; PhCH_2), 3.60–3.50 (m, 2H), 3.50–3.30 (m, 2H), 2.60–2.40 (m, 1H; H-3), 2.40–2.20 (m, 3H; H-3, H-5), 2.20–2.00 ppm (m, 3H; H-5, H-6); ^{13}C NMR (75 MHz, CD_3OD, 25 °C): $\delta = 174.3$, 131.1, 130.7, 129.8, 129.4, 62.0 (*C*Ph), 61.2 (C-4), 55.3 (C-7), 50.5 (C-2), 34.3 (C-5), 31.3 (C-3), 22.0 ppm (C-6); IR (KBr): $\tilde{\nu} = 3435$, 1642 cm^{-1}; MS (ESI$^+$): m/z: 249.1 $(M+1)^+$.

Fmoc-L-Ala-(*R*)- and Fmoc-L-Ala-(*S*)-Azn (10a,b): Operating under nitrogen atmosphere and in the presence of powdered activated molecular sieves, free amino acid **9b** (750 mg, 3 mmol) was dissolved in anhydrous CH_2Cl_2 (20 mL), and BSA (2.65 g, 12 mmol) was added to the stirred solution. The mixture was kept overnight at 25 °C, and then Fmoc-L-Ala-F (1.9 g, 6.0 mmol) was added. After 10 min, the mixture was filtered and the filtrate was concentrated. The crude residue was purified by chromatography on silica gel (CH_2Cl_2/MeOH, 50:1 to 5:1). The resulting mixture of two diastereoisomers **10a**,**b** (1.2 g, 70 %) was separated by flash chromatography (GraceResolv silica cartridges; CH_2Cl_2/MeOH, 10:1) to afford pure **10a** (0.4 g, 25 %; $[\alpha]_{25}^{D} = 43.2°$ ($c = 0.25$, $CHCl_3$)) and **10b** (0.35 g, 20 %; $[\alpha]_{25}^{D} = -107.2°$ ($c = 0.25$, $CHCl_3$)), along with unresolved **10a**,**b** (0.37 g, 22 %).

Preparation of H_2N-L-Ala-Aib-L-Ala-CONH$_2$ on a solid phase: Fmoc-Rink amide resin (250 mg, loading 0.8 mmol g^{-1}) was swollen in CH_2Cl_2 for 20 min. The Fmoc group was removed with piperidine (20 % in DMF, 2×1 mL, 15 + 5 min). Fmoc-Ala-OH (313 mg, 1 mmol) was pre-activated with HOBt/HBTU (0.5 M in DMF, 5 equiv) for 15 min. This solution and DIPEA (1 M in NMP, 10 equiv) were added to the resin and the mixture was stirred for 1 h. Thereafter, the resin was washed with DMF (3 times) and Fmoc cleavage was performed (20 % piperidine in DMF, 15 min + 5 min). The resin was subsequently washed with DMF (6 times). Fmoc-AibOH (325 mg, 1 mmol) was pre-activated with HOBt (135.1 mg, 1 mmol) and DIC (126.2 mg, 1 mmol) in DMF for 20 min. This solution was added to the resin and the mixture was stirred for 3 h. The resin was washed with DMF (3 times) and then the Fmoc group was removed with 20 % piperidine in DMF (15 min + 5 min). The resin was subsequently washed with DMF (6 times). Fmoc-Ala-OH (313 mg, 1 mmol) was pre-activated with HOBt (135.12 mg, 1 mmol) and DIC (126.2 mg, 1 mmol) in DMF for 20 min. This solution was added to the resin and the mixture was stirred for 12 h. The resin was washed with DMF (3 times) and then the Fmoc group was removed with 20 % piperidine in DMF (15 min + 5 min). The resin was subsequently washed with DMF (6 times). The peptide was cleaved from the resin with a mixture of TFA/H_2O/TIS (2 mL/66 μL/88 μL) under stirring for 2 h. The peptide (40 mg, 90 %) was precipitated with a cold mixture of petroleum ether/*t*-butyl methyl ether

(1:1) and purified by RP-HPLC (95% A 2 min, then to 30% A in 30 min, 20 mL min^{-1} flow); ^{1}H NMR (CD_3OD, 25°C): δ = 4.42–4.25 (m, 1H; *CH*Me), 3.98–3.83 (m; *CH*Me), 1.52 (d, J = 6.9 Hz, 3H; Me), 1.50 (s, 6H; Me), 1.31 ppm (d, J = 6.9 Hz, 3H; Me); MS (ESI$^+$): m/z: 245.0 (M+1).

General procedures for the preparation of pentapeptides 11a and 11b: *Method E*: HOAT (27 mg, 0.2 mmol) and EDC (28.4 mg, 0.1 mmol) were added to a solution of dipeptide **10a** (50 mg, 0.1 mmol) in NMP (1.2 mL). The mixture was stirred at 25°C for 1 h, and then the tripeptide H_2N-L-Ala-Aib-L-Ala-$CONH_2$ (73 mg, 0.3 mmol) was added. The reaction mixture was stirred overnight (TLC: CH_2Cl_2/CH_3OH, 10:1). Thereafter, the solvent was removed under vacuum, and the crude mixture was first purified by chromatography on silica gel (CH_2Cl_2/MeOH, 1:0 to 0:1). After RP-HPLC purification (95% A to 30% A gradient over 30 min, 20 mL min^{-1} flow) the product **11a** (20 mg, 30%) and the starting dipeptide **10a** (20 mg, 40%) were collected and freeze-dried. *Method F*: The tripeptide H_2N-L-Ala-Aib-L-Ala-$CONH_2$ (25 mg, 0.1 mmol) and DCC (30 mg, 015 mmol) were added to a solution of dipeptide **10a** or **10b** (50 mg, 0.1 mmol) in CH_2Cl_2 (3 mL). The mixture was stirred at 25°C for 48 h (TLC: CH_2Cl_2/CH_3OH, 10:1). The white solid formed was filtered off and the solvent was removed under vacuum. After RP-HPLC purification under the same conditions of *Method E*, the product **11a** (35 mg, 50%) or **11b** (20 mg, 30%) was obtained and freeze-dried. **11a**: MS (ESI$^+$): m/z: 768.3 (M+1)$^+$; **11b**: MS (ESI$^+$): m/z: 768.4 (M+1)$^+$.

Circular dichroism (CD): The CD spectra of compounds **11a** and **11b** were recorded in MeOH (300 μM solutions) at 25°C (0.1 cm quartz cell, Hellma Suprasil). Spectra were obtained from 195 to 250 nm with a step of 0.1 nm and a collection time per step of 1 s, averaging over three determinations. The spectrum of the solvent was subtracted to eliminate interference from the cell, solvent, and optical equipment. The CD spectra were plotted as mean residue ellipticity θ (degree × cm^2 × dmol^{-1}) versus wavelength λ (nm). Noise reduction was applied using a Fourier-transform filter program from JASCO.

Computational methods: Replica exchange molecular dynamic (REMD) simulations were performed with the Sander module of the Amber11 program package.[30] The parameter sets for the Aib residue were obtained from the RED database,[41] while those for (*R*)/(*S*)-Azn were derived using REDIII software.[42] For the REMD simulation, the number of replicas and the temperature range were selected, on the basis of the number of atoms to be simulated, through the T-REMD server.[43] VMD 1.8.7 software[44] was used for visualizing trajectories, for H-bond analyses, and for obtaining 3D Ramachandran plots. Cluster analyses were performed with ptraj (Amber Tools 1.5)[30] by using the average-linkage algorithm, as suggested by Shao and co-workers,[45] by sampling once every two frames and using the pairwise mass-weighted rmsd between frames as a metric.

Acknowledgements

Funding for this work was provided MIUR (PRIN 2008). Alessandro Contini is grateful to the Consorzio Interuniversitario Lombardo per l'Elaborazione Automatica (CILEA, Via R. Sanzio 4, Segrate, MI) for computational facilities and to Dr. Emanuele Galletta for appreciated collaboration.

[1] J. Tulla-Puche, F. Albericio, in *The Power of Functional Resins in Organic Synthesis* (Eds.: J. Tulla-Puche, F. Albericio), Wiley-VCH, **2008**, 495–527.

[2] C. Pichereau, C. Allary, *Eur. Bio Pharm. Review* **2005**, 88–91.

[3] a) P. Jana, S. Maity, S. K. Maity, D. Haldar, *Chem. Commun.* **2011**, *47*, 2092–2094; b) T. A. Edwards, A. J. Wilson, *Amino Acids* **2011**, *41*, 743–754; c) W. S. Horne, L. M. Johnson, T. J. Ketas, P. J. Klasse, M. Lu, J. P. Moore, S. H. Gellman, *Proc. Natl. Acad. Sci. USA* **2009**, *106*, 14751–14756; d) R. E. Moellering, M. Cornejo, T. N. Davis, C. Del Bianco, J. C. Aster, S. C. Blacklow, A. L. Kung, D. G. Gilliland, G. L. Verdine, J. E. Bradner, *Nature* **2009**, *462*, 182–188; e) E. F. Lee, I. D. Sadowsky, B. J. Smith, P. E. Czabotar, K. J. Peterson-Kaufman, P. M. Colman, S. H. Gellman, W. D. Fairlie, *Angew. Chem.* **2009**, *121*, 4382–4386; *Angew. Chem. Int. Ed.* **2009**, *48*, 4318–4322; f) E. A. Harker, D. S. Daniel, D. A. Guarracino, A. Schepartz, *Bioorg. Med. Chem.* **2009**, *17*, 2038–2046; g) W. D. Wu, S. H. Gellman, *Acc. Chem. Res.* **2008**, *41*, 1231–1232; h) W. S. Horne, S. H. Gellman, *Acc. Chem. Res.* **2008**, *41*, 1399–1408; i) W. S. Horne, M. D. Boersma, M. A. Windsor, S. H. Gellman, *Angew. Chem.* **2008**, *120*, 2895–2898; *Angew. Chem. Int. Ed.* **2008**, *47*, 2853–2856; j) F. Bernal, A. F. Tyler, S. J. Korsmeyer, L. D. Walensky, G. L. Verdine, *J. Am. Chem. Soc.* **2007**, *129*, 2456–2457; k) J. A. Kritzer, R. Zutshi, M. Cheah, F. A. Ran, R. Webman, T. M. Wongjiard, A. Schepartz, *ChemBioChem* **2006**, *7*, 29–31; l) S. H. Gellman, *Acc. Chem. Res.* **1998**, *31*, 173–180.

[4] a) Y. Demizu, M. Doi, M. Kurihara, H. Okuda, M. Nagano, H. Suemune, M. Tanaka, *Org. Biomol. Chem.* **2011**, *9*, 3303–3312; b) E. Gatto, A. Porchetta, L. Stella, I. Guryanov, F. Formaggio, C. Toniolo, B. Kaptein, Q. B. Broxterman, M. Venanzi, *Chem. Biodiversity* **2008**, *5*, 1263–1278; c) M. Tanaka, *Chem. Pharm. Bull.* **2007**, *55*, 349–358; d) C. Toniolo, M. Crisma, F. Formaggio, C. Peggion, Q. B. Broxterman, B. Kaptein, *Biopolymers* **2004**, *76*, 162–176; e) C. Toniolo, M. Crisma, F. Formaggio, C. Peggion, *Biopolymers* **2001**, *60*, 396–419 and references cited therein.

[5] a) E. Longo, A. Moretto, F. Formaggio, C. Toniolo, *Chirality* **2011**, *23*, 756–760 and references cited therein; b) M. Alías, S. Ayuso-Tejedor, J. Fernández-Recio, C. Cativiela, J. Sancho, *Org. Biomol. Chem.* **2010**, *8*, 788–792; c) I. L. Karle, *Biopolymers* **2001**, *60*, 351–365 and references cited therein; d) G. Basu, A. Kuki, *Biopolymers* **1993**, *33*, 995–1000; e) P. Balaram, *Curr. Opin. Struct. Biol.* **1992**, *2*, 845–851.

[6] a) C. Toniolo, A. Polese, F. Formaggio, M. Crisma, J. Kamphuis, *J. Am. Chem. Soc.* **1996**, *118*, 2744–2745; b) P. Enkhbayar, K. Hikichi, M. Osaki, R. H. Kretsinger, N. Matsushima, *Proteins Struct. Funct. Bioinf.* **2006**, *64*, 691–699; c) A. K. Francis, M. Iqbal, P. Balaram, M. Vijayan, *Biopolymers* **1983**, *22*, 1499–1505.

[7] a) Y. Demizu, M. Tanaka, M. Doi, M. Kurihara, H. Okuda, H. Suemune, *J. Pept. Sci.* **2010**, *16*, 621–626; b) K. Wright, J.-F. Lohier, M. Wakselman, J.-P. Mazaleyrat, C. Peggion, F. Formaggio, C. Toniolo, *Biopolymers* **2007**, *88*, 797–806; c) P. Maity, B. König, *J. Pept. Sci.* **2008**, *90*, 8–27; d) M. Crisma, W. M. De Borggraeve, C. Peggion, F. Formaggio, S. Royo, A. I. Jiménez, C. Cativiela, C. Toniolo, *Chem. Eur. J.* **2006**, *12*, 251–260; e) Y. Ohfune, T. Shinada, *Bull. Chem. Soc. Jpn.* **2003**, *76*, 1115–1129; f) C. Toniolo, M. Crisma, F. Formaggio, E. Benedetti, A. Santini, R. Iacovino, M. Saviano, B. Di Blasio, C. Pedone, J. Kamphuis, *Biopolymers* **1997**, *41-44*, 519–522; g) J. Venkatraman, S. C. Shankaramma, P. Balaram, *Chem. Rev.* **2001**, *101*, 3131–3152.

[8] a) S. R. Haynes, S. D. Hagius, M. M. Juban, P. H. Elzer, R. P. Hammer, *J. Peptide Res.* **2008**, *66*, 333–347; b) C. L. Wysong, T. S. Yokum, G. A. Morales, R. L. Gundry, M. L. McLaughlin, R. P. Hammer, *J. Org. Chem.* **1996**, *61*, 7650–7651.

[9] Z. Zhang, H. A. Remmer, D. D. Thomas, C. B. Karim, *Biopolymers* **2007**, *88*, 29–35.

[10] a) M. Bialer, *Epilepsia* **2007**, *48*, 46–48; b) M. N. Ponnuswamy, M. M. Gromiha, S. M. M. Sony, K. Saraboji, *Topics Het. Chem.* **2006**, *3*, 81–147; c) J.-F. Liegeois, J. Bruhwyler, F. Rogister, J. Delarge, *Curr. Med. Chem.* **1995**, *2*, 471–501.

[11] a) W. J. Fairbrother, K. Deshayes, S. Fischer, J. A. Flygare, M. C. Franklin, D. Vucic, PCT Int. Appl., PIXXD2 WO 2004072641A1, **2004**; [*Chem. Abstr.* **2004**, *141*, 218943]; b) O. Murakami, T. Ikebe, I. Hakamata, K. Anami, Jpn. Kokai Tokkyo Koho, Heisei, JKXXAF JP 03034977A 19910214, **1991**; [*Chem. Abstr.* **1991**, *115*, 71603].

[12] S. Murakami, T. Ikebe, I. Hakamada, K. Anami, Eur. Pat. Appl., EPXXDW EP 322779A2 19890705, **1989**; [*Chem. Abstr.* **1990**, *112*, 77239].

[13] S. J. Brickner, J. M. Chen, Z. B. Li, A. Marfat, M. J. Mitton-Fry, M. A. Plotkin, U. D. Reilly, C. Subramanyam, Z. Zhang, S. Robin-

son, U.S. Pat. Appl. Publ., USXXCO US 2008280879A1 20081113, **2008**; [*Chem. Abstr.* **2008**, *149*, 556600].

[14] D. Nunez-Villanueva, M. A. Bonache, L. Infantes, M. T. Garcia-Lopez, M. Martin-Martinez, R. Gonzalez-Muniz, *J. Org. Chem.* **2011**, *76*, 6592–6603.

[15] a) S. Pellegrino, F. Clerici, M. L. Gelmi, *Tetrahedron* **2008**, *64*, 5657–5665; b) M. L. Gelmi, C. Cattaneo, S. Pellegrino, F. Clerici, M. Montali, C. Martini, *J. Org. Chem.* **2007**, *72*, 9811–9814; c) F. Caputo, F. Clerici, M. L. Gelmi, S. Pellegrino, D. Pocar, *Tetrahedron: Asymmetry* **2006**, *17*, 1430–1436; d) F. Caputo, F. Clerici, M. L. Gelmi, S. Pellegrino, T. Pilati, *Tetrahedron: Asymmetry* **2006**, *17*, 61–67; e) F. Caputo, C. Cattaneo, F. Clerici, M. L. Gelmi, S. Pellegrino, *J. Org. Chem.* **2006**, *71*, 8467–8472; f) F. Caputo, F. Clerici, M. L. Gelmi, D. Nava, S. Pellegrino, *Tetrahedron* **2006**, *62*, 1288–1294; g) C. Cabrele, F. Clerici, M. L. Gelmi, R. Gandolfi, F. Molinari, S. Pellegrino, *Tetrahedron* **2006**, *62*, 3502–3508; h) F. Clerici, M. L. Gelmi, S. Pellegrino, T. Pilati, *J. Org. Chem.* **2003**, *68*, 5286–5291; i) F. Clerici, M. L. Gelmi, A. Gambini, *J. Org. Chem.* **2001**, *66*, 4941–4944; j) G. Abbiati, F. Clerici, M. L. Gelmi, A. Gambini, T. Pilati, *J. Org. Chem.* **2001**, *66*, 6299–6304; k) F. Clerici, M. L. Gelmi, D. Pocar, T. Pilati, *Tetrahedron: Asymmetry* **2001**, *12*, 2663–2669; l) F. Clerici, M. L. Gelmi, A. Gambini, D. Nava, *Tetrahedron* **2001**, *57*, 6429–6438; m) F. Clerici, M. L. Gelmi, A. Gambini, *J. Org. Chem.* **2000**, *65*, 6138–6141; n) F. Clerici, M. L. Gelmi, D. Pocar, *J. Org. Chem.* **1999**, *64*, 726–730; o) F. Clerici, M. L. Gelmi, A. Gambini, *J. Org. Chem.* **1999**, *64*, 5764–5767.

[16] A. Avenoza, C. Cativiela, J. H. Busto, M. A. Fernández-Recio, J. M. Peregrina, F. Rodríguez, *Tetrahedron* **2001**, *57*, 545–548.

[17] C. Pedregal, J. Ezquerra, A. Escribano, M. C. Carreño, J. L. G. Ruano, *Tetrahedron Lett.* **1994**, *35*, 2053–2056.

[18] Y. Ohfune, M. Tomita, *J. Am. Chem. Soc.* **1982**, *104*, 3511–3513.

[19] C. Frauenfelder, H.-J. Borschberg, *Helv. Chim. Acta* **2000**, *83*, 1753–1765.

[20] D. Fokas, Z. Wang, *Synth. Commun.* **2008**, *38*, 3816–3822.

[21] M. Jesberger, T. P. Davis, L. Barner, *Synthesis* **2003**, 1929–1958.

[22] R. J. Sundberg, C. P. Walters, J. D. Bloom, *J. Org. Chem.* **1981**, *46*, 3730–3732.

[23] L. A. Carpino, D. Sadat-Aalaee, H. G. Chao, R. H. DeSelms, *J. Am. Chem. Soc.* **1990**, *112*, 9651–9652.

[24] H. R. Kricheldorf, *Justus Liebigs Ann. Chem.* **1972**, *763*, 17–38.

[25] H. Wenschuh, M. Beyermann, R. Winter, M. Bienert, D. Ionescu, L. A. Carpino, *Tetrahedron Lett.* **1996**, *37*, 5483–5486.

[26] Y. Higashimoto, H. Kodama, M. Jelokhani-Niaraki, F. Kato, M. Kondo, *J. Biochem.* **1999**, *125*, 705–712.

[27] A. M. Smith, R. J. Williams, C. Tang, P. Coppo, R. F. Collins, *Adv. Mater.* **2008**, *20*, 37–41.

[28] a) G. L. Millhauser, C. J. Stenland, P. Hanson, K. A. Bolin, F. J. van de Ven, *J. Mol. Biol.* **1997**, *267*, 963–974; b) A. Contini, D. Nava, P. Trimarco, *J. Org. Chem.* **2006**, *71*, 159–166; c) G. L. Millhauser, *Biochemistry* **1995**, *34*, 3873–3877; d) K. Wüthrich, NMR of Proteins and Nucleic Acids, Wiley, New York, **1986**.

[29] J. D. Augspurger, V. A. Bindra, H. A. Scheraga, A. Kuki, *Biochemistry* **1995**, *34*, 2566–2576.

[30] D. A. Case, T. A. Darden, T. E. Cheatham, III, C. L. Simmerling, J. Wang, R. E. Duke, R. Luo, R. C. Walker, W. Zhang, K. M. Merz, B. P. Roberts, B. Wang, S. Hayik, A. Roitberg, G. Seabra, I. Kolossvai, K. F. Wong, F. Paesani, J. Vanicek, J. Liu, X. Wu, S. R. Brozell, T. Steinbrecher, H. Gohlke, Q. Cai, X. Ye, J. Wang, M.-J. Hsieh, G. Cui, D. R. Roe, D. H. Mathews, M. G. Seetin, C. Sagui, V. Babin, T. Luchko, S. Gusarov, A. Kovalenko, P. A. Kollman (2010), AMBER 11, University of California, San Francisco.

[31] Y. Sugita, Y. Okamoto, *Chem. Phys. Lett.* **1999**, *314*, 141–151.

[32] H. Lei, C. Wu, H. Liu, Y. Duan, *Proc. Natl. Acad. Sci. USA* **2007**, *104*, 4925–4930.

[33] J. Mittal, R. B. Best, *Biophys. J.* **2010**, *99*, L26–L28.

[34] D. Paschek, H. Nymeyer, A. E. García, *J. Struct. Biol.* **2007**, *157*, 524–533.

[35] M. Andrec, A. K. Felts, E. Gallicchio, R. M. Levy, *Proc. Natl. Acad. Sci. USA* **2005**, *102*, 6801–6806.

[36] a) H. Yu, X. Daura, W. F. van Gunsteren, *Proteins Struct. Funct. Bioinf.* **2004**, *54*, 116–127; b) R. Bürgi, X. Daura, A. Mark, M. Bellanda, S. Mammi, E. Peggion, W. J. van Gunsteren, *Pept. Res.* **2001**, *57*, 107–118; c) R. Schweitzer-Stenner, W. Gonzales, G. T. Bourne, J. A. Feng, G. R. Marshall, *J. Am. Chem. Soc.* **2007**, *129*, 13095–13109.

[37] M. S. Shell, R. Ritterson, K. A. J. Dill, *J. Phys. Chem. B* **2008**, *112*, 6878–6886.

[38] a) R. B. Best, G. Hummer, *J. Phys. Chem. B* **2009**, *113*, 9004–9015; b) J. Mongan, C. L. Simmerling, J. A. McCammon, D. A. Case, A. Onufriev, *J. Chem. Theory Comput.* **2007**, *3*, 156–169.

[39] G. D. Hawkins, C. J. Cramer, D. G. Truhlar, *J. Phys. Chem.* **1996**, *100*, 19824–19839.

[40] A. Onufriev, D. Bashford, D. A. Case, *Proteins Struct. Funct. Bioinf.* **2004**, *55*, 383–394.

[41] C. Cézard, E. Vanquelef, J. Pecher, P. Sonnet, P. Cieplak, E. Derat, F.-Y. Dupradeau, 236th ACS National Meeting, Philadelphia, PA, USA, August 17 - August 21, 2008.

[42] F.-Y. Dupradeau, A. Pigache, T. Zaffran, C. Savineau, R. Lelong, N. Grivel, D. Lelong, W. Rosanski, P. Cieplak, *Phys. Chem. Chem. Phys.* **2010**, *12*, 7821–7839.

[43] A. Patriksson, D. van der Spoel, *Phys. Chem. Chem. Phys.* **2008**, *10*, 2073–2077.

[44] W. Humphrey, A. Dalke, K. Schulten, *J. Molec. Graphics* **1996**, *14*, 33–38.

[45] J. Shao, S. W. Tanner, N. Thompson, T. E. Cheatham III, *J. Chem. Theory Comput.* **2007**, *3*, 2312–2334.

Received: December 22, 2011
Revised: March 30, 2012
Published online: ■■ ▮▮, 0000

Peptides

S. Pellegrino, A. Contini,* F. Clerici, A. Gori, D. Nava, M. L. Gelmi* ..... ▮▮▮▮–▮▮▮▮

1*H*-Azepine-4-amino-4-carboxylic Acid: A New α,α-Disubstituted Ornithine Analogue Capable of Inducing Helix Conformations in Short Ala-Aib Pentapeptides

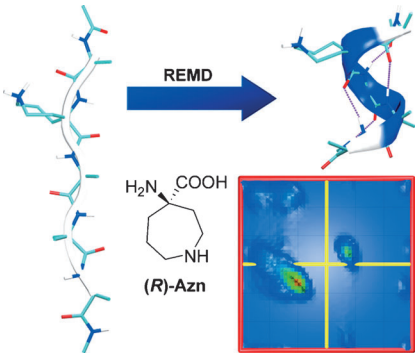

Ahead of the curve: A very efficient synthesis of orthogonally protected 1*H*-azepine-4-amino-4-carboxylic acid (Azn), a conformationally restricted ornithine analogue, was realized. Azn was used to prepare two pentapeptides (L-Ala-(*R*/*S*)-Azn-L-Ala-Aib-L-AlaNH_2). Both computational and spectroscopic data (CD/NMR) revealed the capability of (*R*)-Azn to drive the folding of this short peptide toward a well-defined 3_{10}-helix secondary structure (see figure).